

Sparse Full Configuration Interaction

Lijun Wang^{*,†,‡}

[†]*Center for Scientific Computing, Cavendish Laboratory, University of Cambridge,
Cambridge*

[‡]*Yusuf Hamied Department of Chemistry, University of Cambridge, Cambridge*

E-mail: lw755@cam.ac.uk

Abstract

We propose an efficient deterministic method to calculate the full configuration interaction (FCI) ground state energy. This method leverages the sparseness of the Lanczos basis vectors that span the Krylov subspace associated with the Hamiltonian to rapidly calculate the lowest eigenvalue of the effective Hamiltonian formed in this basis. By iteratively performing the spanning and diagonalization steps, this method is capable of rapidly reaching chemical accuracy for a variety of strongly correlated molecules, including stretched N_2 and C_2 , in merely several tens of iterations. The accuracy is systematically improved by increasing the number of Slater determinants included in a single Lanczos basis vector. To accelerate our algorithm, we implement parallelized sparse matrix-sparse vector multiplication, which features a novel hashing method that establishes a one-to-one correspondence between the set of full configuration Slater determinants and a set of consecutive integers. A near-linear acceleration was observed.

1. Introduction

In order to predict the reactivity of molecules or the properties of quantum materials, one is typically faced with having to solve the quantum system of interest's Schrödinger Equation,

what is thought to be an NP-hard problem that has led to the development of a multitude of approximate classical algorithms. Conceptually, the most straightforward way of solving the Schrödinger Equation is to identify all of the possible, physically-acceptable states of the system and diagonalize the system Hamiltonian formed in this basis of many-body states for its eigenvalues and eigenvectors, which can then be manipulated to obtain its quantum properties. This approach is known as the full configuration interaction (FCI) approach in the chemical literature,^{1,2} and the exact diagonalization (ED) approach in the physical literature.³ Since its computational cost scales combinatorially with the number of orbitals and electrons taken into account, FCI can only be applied to relatively small chemical systems whose wave functions can be expanded in no more than 10^{10} determinants.^{4,5}

Multiple methods have been developed to accurately approximate the FCI ground state energy at much lower cost, making it possible to study previously inaccessible quantum systems, especially the ones that involve strongly correlated electrons. The density matrix renormalization group (DMRG)⁶⁻¹⁰ method, from which a more generalized theory of tensor network states¹¹⁻¹⁸ is derived, provides a compact parametrization of the wave function that only scales polynomially with the system size. Selected CI systematically truncates the exponentially large FCI spaces, only retaining the determinants that have the most significant contribution to the total energy. Beyond the early attempts,¹⁹⁻²⁵ progresses in selected CI in the past decade feature heat-bath CI,²⁶⁻²⁸ adaptive CI,^{29,30} iterative CI,^{31,32} machine learning-based CI,³³ and adaptive sampling CI.^{34,35} Extensive efforts have also been made in stochastically simulating the imaginary time evolution (ITE) $\hat{U}(\tau) = e^{-\hat{H}\tau}$. Auxiliary-field quantum Monte Carlo and its phase-less variant³⁶⁻³⁸ operate within spaces spanned by non-orthogonal determinants. In contrast, the full configuration interaction quantum Monte Carlo (FCIQMC) method³⁹ expands the wave function with a collection of orthogonal determinant walkers, each of which carries either a positive or a negative sign. At discrete time, the dynamics of walkers is governed by $|\Psi(\tau + \delta\tau)\rangle = |\Psi(\tau)\rangle - \delta\tau\hat{H}|\Psi(\tau)\rangle$, and the calculation of the long-time limit $\lim_{\tau \rightarrow \infty} |\Psi(\tau)\rangle$ is enabled by sampling $\hat{H}|\Psi(\tau)\rangle$ at each

time step. This algorithm thus employs an efficient representation of the wave function, and more importantly, circumvents the use of the fixed node approximation^{40–42} that are required in other stochastic ground state algorithms. Multiple modifications to and reformulations of FCIQMC have subsequently been introduced, including initiator approximation,^{43,44} semi-stochastic projection,^{45,46} Chebyshev projector expansion,⁴⁷ and fast randomized iteration.^{48,49} Similar ideas have been applied to devise coupled cluster Monte Carlo.^{50–52} It has also been attempted to sample the intermediate states from the ITE trajectory to construct a basis that enables efficient calculations of isolated excited states, thermal, and spectral properties.⁵³

As observed by Neufeld and Thom, an irksome problem found in FCIQMC is that the “computational effort to reach equilibration can be very significant”.⁵⁴ In practice, 10^5 to 10^6 iterations are required before the energy converges.^{39,43,55} Such a behavior can be understood in terms of the projector’s form. Numerically, the power method (PM) is used to approach the ground state in FCIQMC. Suppose A is an operator, and it has eigenvalues $|\lambda_0| > |\lambda_1| > \dots > |\lambda_N|$. The PM obtains the eigenvector that corresponds to λ_0 by iteratively applying A onto a reasonably chosen trial vector. The convergence rate of PM is determined by $|\lambda_1/\lambda_0|$.⁵⁶ In the projector methods, usually $A = e^{-\delta\tau(\hat{H}-S)}$ (where S is a parameter used for walker population control and $\delta\tau$ a small time step), and the PM’s rate of convergence is $e^{-(E_1-E_0)\delta\tau} \approx 1 - (E_1 - E_0)\delta\tau$, where E_0 and E_1 are the two lowest eigenvalues of H . Since $E_1 - E_0$ is usually of order 10^{-1} a.u., and $\Delta\tau$ ranges from 10^{-3} to 10^{-4} a.u.,^{39,43} the rate of convergence is near-unity in practice, and is arguably a partial reason that FCIQMC-like algorithms are usually costly.

Although new techniques have been proposed to address this shortcoming,^{54,57} new solutions are worth exploring. Here, we propose a deterministic method to approximate the FCI ground state energy more efficiently. We call our method sparse full configuration interaction (SFCI). It is essentially a projector method that also employs ideas from selected CI. In contrast with the FCIQMC family of methods, SFCI uses a process resembling the Lanczos

method to span the search space. It starts with a trial wave function $|v_0\rangle$, and generates a basis that consists of N_L vectors $\{|w_i\rangle\}$ which span the Krylov subspace. However, unlike in the Lanczos method, each SFCI basis vector is truncated with respect to the magnitude of the coefficients, and only contains up to N_d elements. N_d and N_L are both user-defined parameters. With this basis, an N_L -by- N_L effective Hamiltonian T is formed and diagonalized. The eigenvector corresponding to the lowest eigenvalue is then used to construct a new trial wave function for the next round of spanning and diagonalizing. This process is repeated until convergence is reached.

Since we use sparse vectors to represent the Lanczos basis, the efficiency of the whole algorithm relies heavily on that of the sparse matrix-sparse vector multiplication (SpMSpVM). We thus propose and implement a parallel sparse matrix-sparse vector multiplication algorithm. It is based on the algorithm proposed by Azad and Buluc,⁵⁸ which uses a "bucketing" technique to allow different cores to merge their intermediate vectors without communicating with each other. Unlike in this algorithm's original setting, in which non-zero elements of the sparse matrix are explicitly stored, the matrix elements in our application are generated on-the-fly. The absolute index (i.e., the position in the FCI vector) of any determinant is thus unknown, and so the bucketing is hindered. To fill this gap, we introduce an efficient indexing method that establishes a one-to-one correspondence between the FCI determinants and a set of consecutive integers $[0,1,2,\dots,N-1]$. By combining these methods, substantial speedup is achieved. In various tests, our parallelized SpMSpVM implementation achieves speedups of around 12-fold on 32 cores with respect to 2 cores.

This article consists of three parts. First, we introduce the theoretical underpinnings of the SFCI method in Section 2. We next discuss the implementation details of our parallelized sparse matrix-sparse vector multiplication algorithm in Section 3. Finally, in Section 4, we present the results obtained by SFCI on a range of strongly-correlated small molecules, and discuss possible improvements.

2. Method

2.1 Sparse Full Configuration Interaction (SFCI) Iterative Solver

Proposed in 1950,⁵⁹ the Lanczos method has become a powerful tool for finding the extreme eigenvalues and eigenvectors of large sparse self-adjoint matrices. This has led to its widespread application in quantum physics and chemistry, which often seek to obtain ground state wave functions and energies. The Lanczos method is attractive because the number of iterations it requires for accurately approximating the ground state is much smaller than the size of the problem, i.e., the exponentially-scaling dimensionality of the Hilbert space, $\dim(\mathcal{H})$. To our best knowledge, convergence to the ground state is usually achieved within several tens of iterations.

Here, we briefly outline the Lanczos method.⁶⁰ Given a sparse Hamiltonian H and a wave function $|v_0\rangle$, the $N + 1$ -dimensional Krylov subspace is defined as $\mathcal{K}_{N+1}(|v_0\rangle, H) = \text{span}\{v_0, H|v_0\rangle, H^2|v_0\rangle, \dots, H^N|v_0\rangle\}$. The Lanczos method then constructs an orthonormal basis $\{|u_i\rangle\}$ in the Krylov subspace, and diagonalizes the effective Hamiltonian T formed under this basis. In practice, the number of $|u_i\rangle$ required for a converged result (e.g., most commonly, the few eigenvalues that reside at either end of the spectrum) is usually much smaller than the dimension of the Hilbert space.

Such an orthonormal basis is constructed as follows. Given a normalized trial wave function $|v_0\rangle$, let $|u_0\rangle = |v_0\rangle$. $|u_1\rangle$ can next be obtained via a Gram-Schmidt orthogonalization:

$$\begin{aligned} |u'_1\rangle &= H|u_0\rangle - \langle u_0|H|u_0\rangle|u_0\rangle \\ &= H|u_0\rangle - a_0|u_0\rangle \end{aligned} \tag{1}$$

with

$$|u_1\rangle = |u'_1\rangle / \sqrt{\langle u'_1|u'_1\rangle}. \tag{2}$$

Similarly,

$$\begin{aligned}
|u'_2\rangle &= H |u_1\rangle - \langle u_1 | H |u_1\rangle |u_1\rangle - \langle u_0 | H |u_1\rangle |u_0\rangle \\
&= H |u_1\rangle - a_1 |u_1\rangle - b_1 |u_0\rangle \\
|u_2\rangle &= |u'_2\rangle / \sqrt{\langle u'_2 | u'_2\rangle}
\end{aligned} \tag{3}$$

Notice that $|u_3\rangle$ becomes independent of $|u_0\rangle$

$$\begin{aligned}
|u'_3\rangle &= H |u_2\rangle - \langle u_2 | H |u_2\rangle |u_2\rangle - \langle u_1 | H |u_2\rangle |u_1\rangle - \langle u_0 | H |u_2\rangle |u_0\rangle \\
&= H |u_2\rangle - a_2 |u_2\rangle - b_2 |u_1\rangle - 0 \\
|u_3\rangle &= |u'_3\rangle / \sqrt{\langle u'_3 | u'_3\rangle}
\end{aligned} \tag{4}$$

since $\langle u_0 | H |u_2\rangle$ vanishes under the definition in Equations (1) and (3). This leads to a recursive formula to calculate the i^{th} basis vector

$$\begin{aligned}
|u'_i\rangle &= H |u_{i-1}\rangle - \langle u_{i-1} | H |u_{i-1}\rangle |u_{i-1}\rangle - \langle u_{i-2} | H |u_{i-1}\rangle |u_{i-2}\rangle \\
&= H |u_{i-1}\rangle - a_{i-1} |u_{i-1}\rangle - b_{i-1} |u_{i-2}\rangle \\
|u_i\rangle &= |u'_i\rangle / \sqrt{\langle u'_i | u'_i\rangle}
\end{aligned} \tag{5}$$

with

$$\begin{aligned}
a_i &= \langle u_i | H |u_i\rangle \\
b_i &= \langle u_{i-1} | H |u_i\rangle = \sqrt{\langle u_i | u_i\rangle}.
\end{aligned} \tag{6}$$

In other words, T is *tri-diagonal* under the basis $\{|u_i\rangle\}$

$$T_{ij} = \begin{cases} \langle u_i | H |u_j\rangle, & |i - j| \leq 1 \\ 0, & \text{otherwise} \end{cases} \tag{7}$$

With λ_0 being T 's smallest eigenvalue and $x_0 = (c_1, c_2, \dots, c_L)$ its corresponding eigenvector, the approximated ground state wave function is

$$|\Psi_0\rangle = \sum c_i |u_i\rangle \tag{8}$$

and the ground state energy is approximated by

$$E_0 = \frac{\langle \Psi_0 | H | \Psi_0 \rangle}{\langle \Psi_0 | \Psi_0 \rangle}. \quad (9)$$

In our method, the construction of the basis $\{|w_i\rangle\}$ differs slightly from that employed by the Lanczos method: each basis vector $|w_i\rangle$ only contains N_d of the most important determinants. That is, one first obtains

$$\begin{aligned} |u_i\rangle &= H |w_{i-1}\rangle - \langle w_{i-1} | H | w_{i-1} \rangle |w_{i-1}\rangle - \langle w_{i-2} | H | w_{i-1} \rangle |w_{i-2}\rangle \\ &= \sum c_j |D_j\rangle, \quad |c_1| > |c_2| > \dots > |c_n| \end{aligned} \quad (10)$$

in accordance with Equation (5), and truncates the result with respect to the amplitudes

$$\begin{aligned} |w'_i\rangle &= \sum_j^{N_d} c_j |D_j\rangle \\ |w_i\rangle &= |w'_i\rangle / \sqrt{\langle w'_i | w'_i \rangle}. \end{aligned} \quad (11)$$

This restriction avoids the exponential growth in the number of determinants after each application of H . Notice that since all $|w_i\rangle$ are truncated, they are slightly off from being mutually orthogonal. Therefore, the problem of interest becomes a generalized eigenvalue problem, $Tx = \lambda Sx$, where $S_{ij} = \langle w_i | w_j \rangle$. In principle, one could construct a large set of basis vectors and diagonalize T only once. But in practice, we enforce the process to restart after N_L basis vectors $\{|w_1\rangle, |w_2\rangle, \dots, |w_{N_L}\rangle\}$ are collected. It goes as follows: diagonalizing the n^{th} effective Hamiltonian yields an estimated ground state $|\Psi_0^{(n)}\rangle$, which is next truncated down to N_d determinants and used as the the initial basis vector $|w_0^{(n+1)}\rangle$ to form $(n+1)^{\text{th}}$ T . The restarting approach is also widely adopted^{56,61,62} in the application of the Lanczos method. It helps to circumvent the loss of orthogonality of basis as the iteration number increases, which could otherwise introduce spurious solutions that are not physical,^{60,63} as well as to reduce the peak memory usage. Finally, our algorithm halts when $\langle \Psi_0^{(n-1)} | H | \Psi_0^{(n-1)} \rangle -$

$\langle \Psi_0^{(n)} | H | \Psi_0^{(n)} \rangle$ falls below a threshold ϵ .

2.2 Sparse Matrix Sparse Vector Multiplication in Parallel

Since all wave functions in SFCI are represented by sparse vectors, an efficient sparse matrix-sparse vector multiplication is desirable. However, although parallel sparse matrix-dense vector multiplication (SpMVM) has been implemented in various libraries, shifting to the case of sparse matrix-sparse vector multiplication (SpMSpVM) requires extra care. We now demonstrate a novel SpMSpVM algorithm that particularly suits problems in determinant spaces. We restrict our discussion to the way the algorithm would function on a shared-memory machine in this article. As will be shown later, migrating this algorithm to a distributed memory system is straightforward.

We implement the parallel SpMSpVM algorithm based on the "bucketing strategy" proposed by Azad and Buluc.⁵⁸ The advantage of such a design is that it enables all available computational resources to simultaneously work on the merging part of the SpMSpVM calculation. Suppose the problem of interest is $Ax = y$, where A is a sparse matrix and x, y are sparse vectors. We represent a sparse vector as a set of 2-tuples (i, α_i) , where α_i is the non-zero element and i its index within the array (see Figure 1 for a depiction). A sparse matrix is instead a set of 3-tuples (i, j, c_{ij}) , where i, j are the row and column indices, and c_{ij} the non-zero element. There are two major steps in a SpMSpVM calculation. First, for each (i, α_i) in x , all of its connected product 2-tuples $\{(k, \alpha_i c_{ki})\}$ are generated by going through all 3-tuples with matching indices $\{(k, i, c_{ki})\}$ in A . We call those 2-tuples generated from x *intermediate elements*. Second, the set of intermediate elements is merged, i.e., all 2-tuples with identical indices $(i, \alpha_i^1), (i, \alpha_i^2), (i, \alpha_i^3)$, etc., are merged into a single 2-tuple $(i, \sum_j \alpha_i^j)$. The merged set of intermediate elements is just the resultant sparse vector y . Parallelizing step 1 is straightforward, as one could assign each available CPU core with a segment of x and generate the intermediate elements simultaneously. It is less obvious how step 2 can be executed in parallel, but this is where the bucketing becomes advantageous. As shown

in Figure 1, the intermediate elements are distributed across buckets based on their indices. Each bucket can be merged by different CPU cores without communication between them. Finally, the merged buckets are concatenated to form the result y .

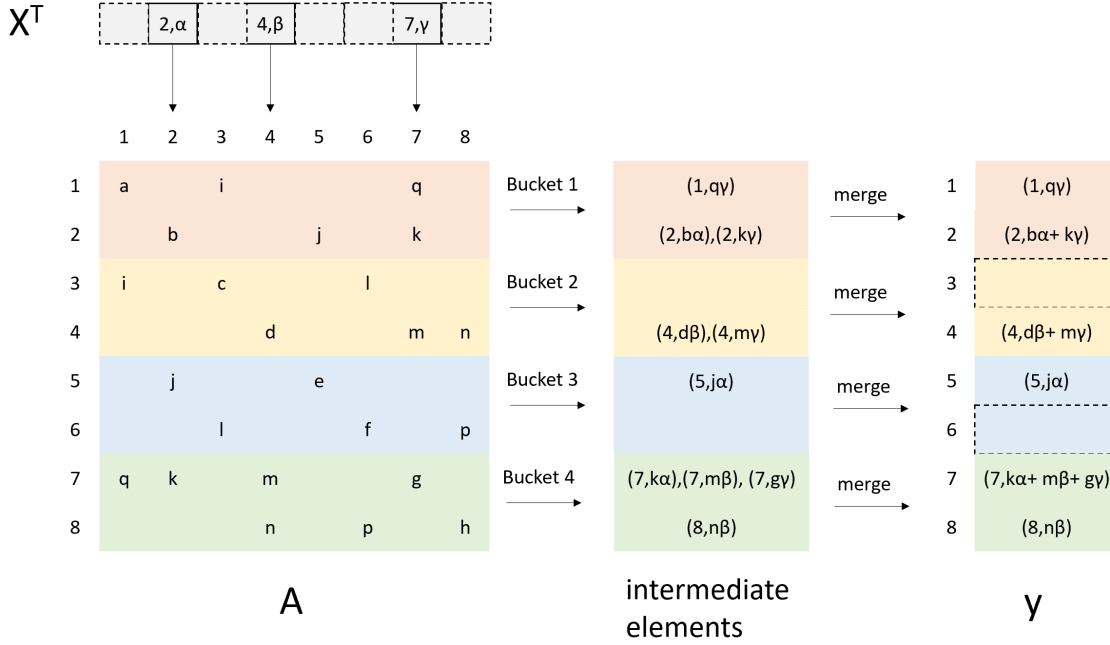


Figure 1: Demonstration of the bucketing in a SpMSpVM calculation. Dashed blocks in x^T and y stands for zero elements. For clarity, the sparse matrix A is shown as a square rather than as 3-tuples. Buckets are labeled with different colors. Notice that, without the bucketing, all intermediate elements have to be merged by 1 core, but 4 cores can now work on the merging simultaneously with bucketing.

In practice, when the input vector x has a large number of elements, N_T cores will independently calculate their own segments to generate all of the intermediate elements. To avoid a data race, each core is assigned an independent copy of the buckets. When all intermediate elements are generated, these local buckets are brought together to form the final set of buckets. A sort-and-merge scheme is used to merge each bucket: first, all elements in the bucket are sorted with respect to the determinant, so that the coefficients of a single determinant are brought together. A scan from the beginning to the end will next merge these coefficients. We use the introspective sort as the sorting method, whose average and worst case complexity are both $O(n \log n)$.⁶⁴ The complexity of the scanning step is the

typical $O(n)$.

In FCI, the matrix elements are calculated before the optimization starts. First, the complete set of FCI determinants is generated, so that any determinant's index within a dense FCI vector can be determined. One may create for later convenience a hash table h with the determinant as its key and index its value. Next, for all determinants $|D_i\rangle$, with i being $|D_i\rangle$'s index in the FCI vector, all its connected determinants $|D_j\rangle$ are calculated. j can be easily found using the previously built hash table h . All 3-tuples $(i, j, \langle D_i | H | D_j \rangle)$ are finally stored in the sparse matrix data structure, which will be used later in sparse matrix-dense vector multiplications. In contrast, since it is impossible to explicitly store all matrix elements for large systems, matrix elements must be generated on the fly. That is, given any determinant $|D\rangle$, all of its connected determinants $|D_\alpha\rangle$, as well as the corresponding matrix elements $\{\langle D_\alpha | H | D \rangle\}$, are calculated. There is, however, no way to know a determinant's index when the system becomes large, since it is impossible to explicitly generate an FCI vector. The bucketing thus breaks down for large systems.

To tackle this problem, we introduce a novel hashing method to enable bucketing under matrix-free SpMSpVM in determinant spaces. Essentially, such a method establishes a one-to-one correspondence between a set of FCI determinants $\{|D_1\rangle, |D_2\rangle, \dots, |D_N\rangle\}$, and a set of consecutive integers $\{0, 1, 2, \dots, N - 1\}$. Suppose $|D\rangle = |\chi_1\chi_2\dots\chi_M\rangle$, where χ_i is the orbital index occupied by the i th electron and ranges from $[1, N_{orb}]$. The hash value of $|D\rangle$ is calculated using the following formula:

$$h(|D\rangle) = \sum_{i=1}^M \binom{\chi_i - 1}{i} \quad (12)$$

in which all $\binom{n}{k}$ values with n smaller than k are set to 0 for convenience.

Such a formula is derived from two observations. First, given a properly chosen "initial" determinant, all determinants in the FCI space can be enumerated *recursively*. That is, given any bit string that represents a determinant, its unique successor can be found by a function g . The only exception is the "final" determinant, which has no successor. To that end, we

define the initial determinant in any system as 11..1100..000, in which all 1-bits are flushed to the left. Consequently, the final determinant can be defined as 00..001..11, in which all 1-bits are flushed to the right. We then define function g as follows. For any determinant written in bit string form, g :

Scan from the left all 1-bits in the bit string. If a 1-bit has a 0-bit as its right neighbor, flush all 1-bits on its left to the left, swap these two bits, and return the new bit string as the successor; if none of the 1-bits have a 0-bit as a right neighbor, the final determinant has been reached.

In the table below, we use a system with 6 orbitals and 3 electrons to demonstrate how to enumerate the entire FCI space using g starting with the initial determinant. We call the

Table 1: Generation of the FCI space of a (6o,3e) system via g .

$$\begin{array}{cccccccc}
111000 & \xrightarrow{g} & 110100 & \xrightarrow{g} & 101100 & \xrightarrow{g} & 011100 & \xrightarrow{g} & 110010 \\
\xrightarrow{g} & 101010 & \xrightarrow{g} & 011010 & \xrightarrow{g} & 100110 & \xrightarrow{g} & 010110 & \xrightarrow{g} & 001110 \\
\xrightarrow{g} & 110001 & \xrightarrow{g} & 101001 & \xrightarrow{g} & 011001 & \xrightarrow{g} & 100101 & \xrightarrow{g} & 010101 \\
\xrightarrow{g} & 001101 & \xrightarrow{g} & 100011 & \xrightarrow{g} & 010011 & \xrightarrow{g} & 001011 & \xrightarrow{g} & 000111
\end{array}$$

above enumerating process a "g-chain" for later convenience. Now, it is obvious that the distance from the initial determinant, i.e. how many times g has been applied, uniquely defines any determinant in the FCI space, and the value of distance can therefore be used as the index of the corresponding determinant.

Second, to calculate the distance, observe that it can be further decomposed into the contributions made by each 1-bit. We use the following example to demonstrate how to calculate these contributions. Consider the determinant in the bit-string form 101010. The rightmost 1-bit occupies orbital 5, meaning that before arriving at the current determinant, one must, at least, pass through all determinants in the g-chain with 3 electrons occupying the first 4 orbitals from the initial determinant. We thus take the contribution from this 1-bit as $\binom{4}{3} = 4$. Next, the second 1-bit occupies orbital 3. To reach the configuration with the third electron occupying orbital 5 and second electron orbital 3, one has to pass

through all determinants with the first 2 electrons occupying the first 2 orbitals and the third electron in orbital 5, whose total number is $\binom{2}{2} = 1$. Finally, the first electron is not shifted from its initial orbital, yielding a contribution $\binom{0}{1} = 0$. The distance, of 101010 is therefore $4 + 1 + 0 = 5$, which we take as its hash value. This can be verified in the g-chain shown above, in which the initial determinant has hash value 0. A complete list of the hash values of this system is given in Table 2.

Table 2: Hash values of all determinants with 6 orbitals and 3 electrons

$h(111000\rangle) = \binom{0}{1} + \binom{1}{2} + \binom{2}{3} = 0$	$h(110001\rangle) = \binom{0}{1} + \binom{1}{2} + \binom{5}{3} = 10$
$h(110100\rangle) = \binom{0}{1} + \binom{1}{2} + \binom{3}{3} = 1$	$h(101001\rangle) = \binom{0}{1} + \binom{2}{2} + \binom{5}{3} = 11$
$h(101100\rangle) = \binom{0}{1} + \binom{2}{2} + \binom{3}{3} = 2$	$h(011001\rangle) = \binom{1}{1} + \binom{2}{2} + \binom{5}{3} = 12$
$h(011100\rangle) = \binom{1}{1} + \binom{2}{2} + \binom{3}{3} = 3$	$h(100101\rangle) = \binom{0}{1} + \binom{3}{2} + \binom{5}{3} = 13$
$h(110010\rangle) = \binom{0}{1} + \binom{1}{2} + \binom{4}{3} = 4$	$h(010101\rangle) = \binom{1}{1} + \binom{3}{2} + \binom{5}{3} = 14$
$h(101010\rangle) = \binom{0}{1} + \binom{2}{2} + \binom{4}{3} = 5$	$h(001101\rangle) = \binom{1}{1} + \binom{2}{2} + \binom{5}{3} = 15$
$h(011010\rangle) = \binom{1}{1} + \binom{2}{2} + \binom{4}{3} = 6$	$h(100011\rangle) = \binom{0}{1} + \binom{4}{2} + \binom{5}{3} = 16$
$h(100110\rangle) = \binom{0}{1} + \binom{3}{2} + \binom{4}{3} = 7$	$h(010011\rangle) = \binom{1}{1} + \binom{4}{2} + \binom{5}{3} = 17$
$h(010110\rangle) = \binom{1}{1} + \binom{3}{2} + \binom{4}{3} = 8$	$h(001011\rangle) = \binom{2}{1} + \binom{4}{2} + \binom{5}{3} = 18$
$h(001110\rangle) = \binom{1}{1} + \binom{2}{2} + \binom{4}{3} = 9$	$h(000111\rangle) = \binom{1}{1} + \binom{4}{2} + \binom{5}{3} = 19$

For any determinant $|D\rangle$ that needs to be bucketed, its hash value $h(|D\rangle)$ is used to determine the bucket to which it belongs. Given the pre-defined bucket size N_B (i.e. the number of indices it contains), the bucket index of $|D\rangle$ is the floor of $\frac{h(|D\rangle)}{N_B}$, i.e., $\lfloor \frac{h(|D\rangle)}{N_B} \rfloor$.

3. Computational Details

In this work, we consider molecular Hamiltonians that contain up to double excitations. We use MolPro⁶⁵ to calculate the restricted Hartree-Fock (RHF) determinant as well as the associated electron-electron integrals. The RHF determinant is used as the trial wave function. Matrix elements $\langle D_i | H | D_j \rangle$ in the SFCI calculation are generated via our own implementation in C++. We use a 64-bit unsigned integer in which a 1-bit corresponds to an occupied spin orbital, while a 0-bit an unoccupied spin orbital to represent determinants. Though at this point such a representation can only accommodate determinants with no

more than 64 spin orbitals, this representation can be generalized by, for instance, using more than one integer to represent a single determinant. Additionally, in all of our calculations, we compute the bucketing indices only with respect to the spin-up section of the bit-string. For closed-shell systems, this can reduce the time cost by a factor of 2. Finally, all of our numerical experiments are carried out on a single node containing two 2.80GHz Intel Xeon Gold 6242 CPUs, with 32 cores in total. All cores are used in the experiments unless otherwise specified.

In practice, we introduce an extra parameter to accelerate the calculation of $H|u_i\rangle$, which is the most expensive part of the whole SFCI routine. As described in the previous sections, the merged intermediate vectors from different buckets in $H|u_i\rangle$ are concatenated into one vector $|v\rangle$, and the most important N_d determinants are picked out to form $|u_{i+1}\rangle$. This requires sorting the whole $|v\rangle$ vector. However, sorting $|v\rangle$ can be expensive, since its length can be a thousand times larger than that of $|u_i\rangle$ in practice. We therefore introduce ϵ as the threshold for incorporating the determinants into $|v\rangle$. No determinant in the intermediate vectors with coefficient amplitude below ϵ is incorporated into $|v\rangle$. Such a truncation in principle influences the values of all $T_{ij}, j < i$, but in the experiments, we find that it has no visible effect on the accuracy of SFCI. It is also noteworthy that, in some cases, an ϵ that is too small can lead to non-physical solutions and complicate convergence. In all tests below, we use $\epsilon = 5 \times 10^{-5}$.

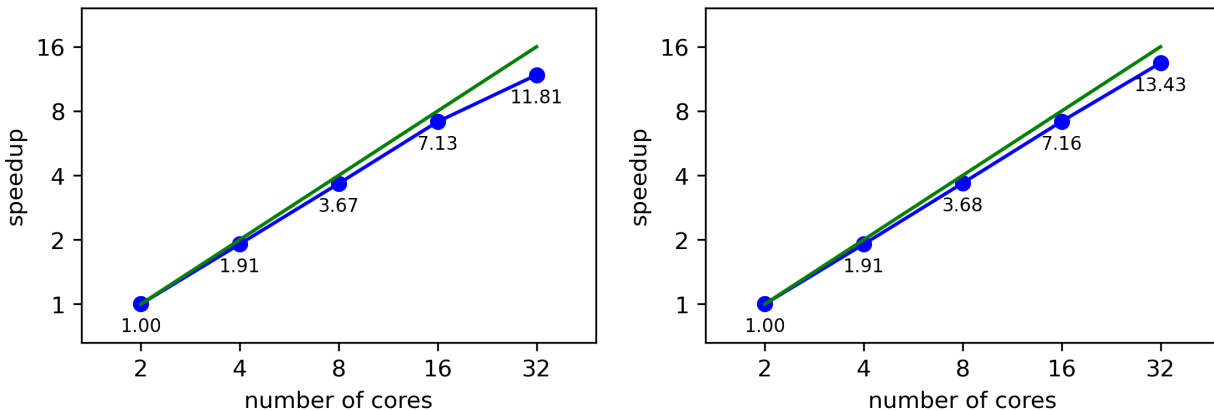
The source code that implements the above can be accessed at.⁶⁶

4. Results

4.1 Sparse-Matrix Sparse-Vector Acceleration

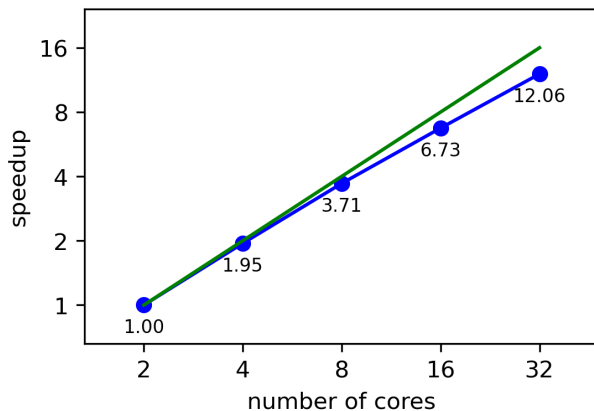
We first demonstrate the acceleration achieved by our SpMSpVM algorithm. Figure 2 shows the acceleration ratios of a single SpMSpVM calculation with different numbers of cores for different systems. We use 2 cores as the baseline since bucketing is meaningless on 1 core.

The tests manifest clearly that our SpMSpVM implementation is able to achieve a similar, near linear speedup for different Hamiltonians and input vector sizes.



(a) C_2 , cc-pVDZ, $N_d = 4 \times 10^5$

(b) C_2 , cc-pVDZ, $N_d = 8 \times 10^5$ dets



(c) N_2 , cc-pVDZ, $N_d = 4 \times 10^5$ dets

Figure 2: Relative parallel SpMSpVM speedup for different molecular systems. The blue dots represent the acceleration ratio relative to 2 cores, while the green line is the ideal linear scaling with respect to the core number. The three cases that have been plotted are: C_2 using the cc-pVDZ basis with input vector of size $N_d = 4 \times 10^5$, C_2 using the cc-pVDZ basis with input vector of size $N_d = 8 \times 10^5$, and N_2 using the cc-pVDZ basis, with input vector $N_d = 4 \times 10^5$.

4.2 Convergence of SFCI Algorithm with Respect to the Number of Determinants and Basis Size

We further test the convergence of SFCI, as well as how parameters N_d and N_L impact that convergence. Table 3 provides the SFCI results for C_2 and N_2 , multiply-bonded molecules with known FCI benchmark energies. C_2 is analyzed at its equilibrium geometry (bond distance of 1.27273 Å), while N_2 is analyzed in both its equilibrium (bond distance of 1.09397 Å) and stretched (bond distance of 2.22180 Å) geometry. The above geometries are from Ref.³⁹ In all calculations, N_L (i.e., the dimensionality of the effective Hamiltonian) is fixed at 10. It can be seen that 1 mHa accuracy is easily obtained in all cases within spaces that are merely 1% as large as the FCI spaces.. For C_2 , the best SFCI energy is 0.13 mHa above the FCI result. For N_2 , the best results are 0.29 mHa and 0.43 mHa above the FCI results for the equilibrium and stretched geometries, respectively. To give an idea of the computation time, C_2 with $N_d = 4 \times 10^5$ takes 10 minutes, while N_2 in equilibrium with $N_d = 6 \times 10^5$ takes 14 minutes. It is also clear that as N_d increases, the error of the converged result decreases in all three cases. Also, the size of the resulting wave function, $|\phi_0\rangle$, is roughly proportional to N_d , indicating that increasing N_d can lead to a larger solution space.

SFCI may also be observed to converge rapidly with respect to the iteration number N_I . We define the iteration number as how many times SpMSPVM is applied before convergence is achieved, which is simply N_L times the number of effective Hamiltonians that have been diagonalized. As shown in Table 3, the N_I required for convergence never exceeds 100 in all of our experiments, indicating that SFCI has successfully inherited the Lanczos method’s advantage of rapid convergence.

Table 3: SFCI energies as a function of the number of determinants and iterations. C_2 is studied in its equilibrium geometry while N_2 is studied in both its equilibrium and stretched geometries in the cc-pVDZ basis set with a frozen core. This yields a (26o,8e) configuration for C_2 , and a (26,10e) configuration for N_2 . The size of the FCI spaces in the D_{2h} point group are 2.79×10^7 and 5.41×10^8 , respectively. The FCI result for C_2 is obtained via MolPro, while those for N_2 in its equilibrium and stretched geometries are obtained from References⁵ and,⁶⁷ respectively. Energies are in units of Hartrees.

System	$N_d/10^5$	size of $ \phi_0\rangle/10^5$	N_I	E_{SFCI}	E_{FCI}	$E_{FCI} - E_{SFCI}/\text{mHa}$
C ₂	2	5.8	50	-75.729413	-75.729852	0.439
	4	10.4	50	-75.729664		0.188
	6	12.0	40	-75.729667		0.184
	8	13.7	50	-75.729696		0.155
	10	18.2	50	-75.729717		0.135
N ₂ equilibrium	2	5.5	40	-109.275647	-109.276527	0.88
	4	11.3	40	-109.276097		0.430
	6	15.9	40	-109.276234		0.292
	8	14.8	30	-109.276235		0.292
	10	17.8	30	-109.276251		0.276
N ₂ stretched	2	6.4	90	-108.96454	-108.96695	2.409
	4	12.6	80	-108.96576		1.189
	6	19.0	80	-108.96622		0.729
	8	24.6	80	-108.96644		0.509
	10	24.2	80	-108.96651		0.43

We observe that, in comparison to N_d , N_L has a much less visible impact on the accuracy of the converged results. In the applications of the Lanczos method, a larger N_L means more degrees of freedom for variation, resulting in faster convergence.⁶⁰ However, we observe that neither the speed of convergence nor the SFCI algorithm’s accuracy is significantly changed by varying N_L . Table 4 shows the converged energies and iteration numbers for different N_L for the C₂ cc-pVDZ system. Notice that different N_L only yield 10^{-2} mHa differences in the converged energies, and small differences in the number of iterations needed for convergence. This suggests that using a relatively small N_L is not only economical, but reasonably accurate.

Table 4: SFCI results of C₂ cc-pVDZ with different N_L with N_d is fixed to 4×10^5 . In contrast to one may expect, increasing N_L benefits neither the algorithm’s accuracy nor its speed of convergence.

N_L	E_{SFCI}	N_I
5	-75.729646	50
10	-75.729683	50
15	-75.729689	75
20	-75.729665	80

4.3 Quantum Chemical Benchmarks

We finally test SFCI on several more challenging systems. Table 2 shows the SFCI results for systems for which FCI results are absent, as well as existing results obtained by other methods. In all cases, $N_L = 10$, except for F_2 , for which we use $N_L = 5$. For Ne, CO, and C_2 with all of its electrons fully correlated, SFCI results are all within 0.5 mHa of the existing DMRG or FCIQMC results. On the other hand, F_2 stands as an example that is overly challenging for FCI calculations. For F_2 in its equilibrium geometry with all of its electrons correlated in the cc-pVDZ basis, its FCI space size reaches 5.96×10^{12} under the D_{2h} point group. With $N_d = 6 \times 10^5$, its SFCI energy is -199.102153 Ha, which is 1 mHa lower than the CCSD(t) energy of $E_{CCSD(t)} = -199.101154$ Ha. The size of the resulting wave function is 1.24×10^6 determinants. In comparison, under a slightly different geometry, the ASCI method yields $E_{ASCI} = -199.101763$ Ha with 10^6 determinants and $E_{CCSD(t)} = -199.101481$ Ha, a discrepancy of 0.28 mHa.³⁵ However, the bare ASCI result is significantly improved by the second order Epstein-Nesbet correction, which yields an energy that is 1.864 mHa lower than the CCSD(t) result.³⁵ This suggests that combining perturbative corrections with SFCI may further improve the latter’s accuracy, a point for further future exploration. The longest computation among these examples is F_2 with $N_d = 6 \times 10^5$, which took 85 minutes. This further attests to the rapid convergence of SFCI.

Table 5: SFCI energies relative to those obtained from other methods. The geometries used for the diatomic molecules are: CO ($r = 1.1448 \text{ \AA}$), C_2 ($r = 1.24253 \text{ \AA}$), and F_2 ($r = 1.412 \text{ \AA}$). For Ne, C_2 , and F_2 , all electrons (AE) are correlated, while for CO, the core electrons are frozen. The resultant configurations are : Ne(23o,10e), CO(26o,10e), C_2 (28o,12e), and F_2 (28o,18e). The D_{2h} point group is used for all species presented except for CO, which is given in the C_{2v} point group. The resultant sizes of the FCI spaces for these systems are: Ne (1.4×10^8 determinants), CO(1.08×10^9 determinants), C_2 (1.77×10^{10} determinants), and F_2 (5.96×10^{12} determinants). The FCIQMC result for CO is obtained from ref.³⁹ The DMRG result for Ne is obtained from,⁵³ and for C_2 from.⁶⁸ M in the table denotes the bond dimension used for the DMRG calculations. The CCSD(t) result for F_2 is calculated via MolPro.

System	$N_d / 10^5$	E_{SFCI}	E_{DMRG}	E_{FCIQMC}	$E_{CCSD(t)}$	N_I
Ne, AE	2	-128.711461	-128.71147 (M=500)			30
CO	4	-113.055552		-113.05644		40
	8	-113.056045				50
	12	-113.056066				30
C_2 , AE	4	-75.731555	-75.731958 (M=4000)			80
	8	-75.731715				100
F_2 , AE	2	-199.101305			-199.101154	70
	4	-199.1016715				80
	6	-199.102153				80

We now briefly compare SFCI and Krylov-projected FCIQMC (KP-FCIQMC),⁵³ which appears similar at first glance. Besides being a deterministic method, SFCI differs from KP-FCIQMC in both its projection approach as well as the basis chosen. In KP-FCIQMC, an FCIQMC-style projector $\hat{P} = 1 - \delta\tau(H - S)$ is used to define the Krylov subspace \mathcal{K} , and the basis for constructing the effective H is of the form $\{\hat{P}^n |\psi_0\rangle\}$, which is far from being orthogonal. But in SFCI, H is used as in the Lanczos method to define \mathcal{K} , and the computational basis is designed to be orthogonal, though the truncation process introduces slight nonorthogonality in practice. Regarding the ground state calculation, this setting arguably makes SFCI more efficient. Also, SFCI and KP-FCIQMC adopt slightly different techniques for curtailing the increasing linear dependence of the basis vectors that appear during late stages of the algorithm. As shown above, SFCI restricts the number of basis

vectors to a relatively small number and restarts its spanning and diagonalization multiple times; in contrast, KP-FCIQMC samples from the Krylov vectors with linearly increasing distances between selections, so that the vectors in the later stage of the algorithm, which have increasingly larger overlap with the previous ones, are less likely to be selected.

Improving upon this algorithm by parallelizing SFCI over multiple compute nodes is straightforward, and we briefly outline the strategy here. Suppose N nodes are collaboratively carrying out a SpMSpVM calculation on the input wave function $|x\rangle$. Each node computes a segment of $|x\rangle$ simultaneously, and let $|y_i\rangle$ denote the resultant sparse vector from node i . Now, all $|y_i\rangle$ have to be merged and truncated into one single sparse vector. However, it is possible that a single node's memory is insufficient to accommodate all $|y_i\rangle$. An alternative approach is to merge $|y_i\rangle$ via a reduction tree. The reduction continues until only one active node remains. At each layer, the inter-node communications and the merging-and-truncation steps of all pairs take place simultaneously. The total time cost of the reduction will be $\log(N)$ times the time cost of a single layer. The calculation of the effective Hamiltonian T and the overlap matrix S is finally carried out on the master node.

We now discuss a few possibilities for future development. We notice that some recent advances in the selected CI method may also further accelerate SFCI. For example, since the current version of SFCI generates all single and double excitations of the reference determinants, incorporating heat-bath CI's efficient selection method²⁶ will significantly reduced the time consumed in sorting and merging. Semi-stochastic projection^{45,55} may also lead to further improvements in efficiency. It is furthermore possible to find low-lying excited state energies via SFCI. In theory, the only modification required, is to properly project out all previously found eigenvectors in H_{eff} when solving for the i^{th} excited state.⁶⁹

5. Conclusions

We have proposed and implemented an efficient deterministic method to approximate the FCI energy with modest computation resources. Compared to FCIQMC-style methods, SFCI constructs a Lanczos-like basis to search for the ground state energy, thus requiring far fewer iterations to converge. We have shown that SFCI is capable of obtaining highly accurate ground state energies for various strongly correlated systems with FCI spaces of up to 5.96×10^{12} determinants. Our novel indexing function as well as our implementation of the parallel sparse matrix and sparse vector multiplication have enabled us to achieve the above results in a matter of an hour. We believe that, in combination with various other techniques, the efficiency and the accuracy of SFCI can be further improved, making it possible to study a wide variety of challenging problems in quantum many body physics and chemistry.

Data Availability

All codes, scripts, and data needed to reproduce the results in this paper are available online at: <https://github.com/wlj89/SFCI>.

Acknowledgements

The author is greatly indebted to Brenda Rubenstein for support and guidance, and thanks Alex Thom for helpful discussions. This research was conducted using computational resources and services at the Center for Computation and Visualization, Brown University.

References

- (1) Knowles, P.; Handy, N. A new determinant-based full configuration interaction method. *Chemical Physics Letters* **1984**, *111*, 315–321.
- (2) Knowles, P. J.; Handy, N. C. A determinant based full configuration interaction program. *Computer Physics Communications* **1989**, *54*, 75–83.
- (3) Weiße, A.; Fehske, H. In *Computational Many-Particle Physics*; Fehske, H., Schneider, R., Weiße, A., Eds.; Springer Berlin Heidelberg: Berlin, Heidelberg, 2008; pp 529–544.
- (4) Rossi, E.; Bendazzoli, G. L.; Evangelisti, S.; Maynau, D. A full-configuration benchmark for the N₂ molecule. *Chemical Physics Letters* **1999**, *310*, 530–536.
- (5) Gan, Z.; Grant, D. J.; Harrison, R. J.; Dixon, D. A. The lowest energy states of the group-IIIA–group-VA heteronuclear diatomics: BN, BP, AlN, and AlP from full configuration interaction calculations. *The Journal of Chemical Physics* **2006**, *125*, 124311.
- (6) White, S. R. Density matrix formulation for quantum renormalization groups. *Phys. Rev. Lett.* **1992**, *69*, 2863–2866.
- (7) White, S. R.; Martin, R. L. Ab initio quantum chemistry using the density matrix renormalization group. *The Journal of Chemical Physics* **1999**, *110*, 4127–4130.
- (8) Sharma, S.; Chan, G. K.-L. Spin-adapted density matrix renormalization group algorithms for quantum chemistry. *The Journal of Chemical Physics* **2012**, *136*, 124121.
- (9) Zgid, D.; Nooijen, M. The density matrix renormalization group self-consistent field method: Orbital optimization with the density matrix renormalization group method in the active space. *The Journal of Chemical Physics* **2008**, *128*, 144116.

- (10) Kurashige, Y.; Yanai, T. High-performance ab initio density matrix renormalization group method: Applicability to large-scale multireference problems for metal compounds. *The Journal of Chemical Physics* **2009**, *130*, 234114.
- (11) Olivares-Amaya, R.; Hu, W.; Nakatani, N.; Sharma, S.; Yang, J.; Chan, G. K.-L. The ab-initio density matrix renormalization group in practice. *The Journal of Chemical Physics* **2015**, *142*, 034102.
- (12) Keller, S.; Dolfi, M.; Troyer, M.; Reiher, M. An efficient matrix product operator representation of the quantum chemical Hamiltonian. *The Journal of Chemical Physics* **2015**, *143*, 244118.
- (13) Chan, G. K.-L.; Keselman, A.; Nakatani, N.; Li, Z.; White, S. R. Matrix product operators, matrix product states, and ab initio density matrix renormalization group algorithms. *The Journal of Chemical Physics* **2016**, *145*, 014102.
- (14) Szalay, S.; Pfeiffer, M.; Murg, V.; Barcza, G.; Verstraete, F.; Schneider, R.; Legeza, O. Tensor product methods and entanglement optimization for ab initio quantum chemistry. *International Journal of Quantum Chemistry* **2015**, *115*, 1342–1391.
- (15) Murg, V.; Verstraete, F.; Schneider, R.; Nagy, P. R.; Legeza, O. Tree Tensor Network State with Variable Tensor Order: An Efficient Multireference Method for Strongly Correlated Systems. *Journal of Chemical Theory and Computation* **2015**, *11*, 1027–1036, PMID: 25844072.
- (16) Larsson, H. R.; Zhai, H.; Gunst, K.; Chan, G. K.-L. Matrix Product States with Large Sites. *Journal of Chemical Theory and Computation* **2022**, *18*, 749–762.
- (17) Marti, K. H.; Bauer, B.; Reiher, M.; Troyer, M.; Verstraete, F. Complete-graph tensor network states: a new fermionic wave function ansatz for molecules. *New Journal of Physics* **2010**, *12*, 103008.

- (18) Gunst, K.; Verstraete, F.; Wouters, S.; Legeza, O.; Van Neck, D. T3NS: Three-Legged Tree Tensor Network States. *Journal of Chemical Theory and Computation* **2018**, *14*, 2026–2033.
- (19) Buenker, R. J.; Peyerimhoff, S. D. Individualized configuration selection in CI calculations with subsequent energy extrapolation. *Theoretica chimica acta* **1974**, *35*, 33–58.
- (20) Buenker, R. J.; Peyerimhoff, S. D. Energy extrapolation in CI calculations. *Theoretica chimica acta* **1975**, *39*, 217–228.
- (21) Huron, B.; Malrieu, J. P.; Rancurel, P. Iterative perturbation calculations of ground and excited state energies from multiconfigurational zeroth-order wavefunctions. *The Journal of Chemical Physics* **2003**, *58*, 5745–5759.
- (22) Evangelisti, S.; Daudey, J.-P.; Malrieu, J.-P. Convergence of an improved CIPSI algorithm. *Chemical Physics* **1983**, *75*, 91–102.
- (23) Meller, J.; Heully, J.; Malrieu, J. Size-consistent self-consistent combination of selected CI and perturbation theory. *Chemical Physics Letters* **1994**, *218*, 276–282.
- (24) Olsen, J.; Roos, B. O.; Jørgensen, P.; Jensen, H. J. A. Determinant based configuration interaction algorithms for complete and restricted configuration interaction spaces. *The Journal of Chemical Physics* **1988**, *89*, 2185–2192.
- (25) Angeli, C.; Cimiraglia, R.; Persico, M.; Toniolo, A. Multireference perturbation CI I. Extrapolation procedures with CAS or selected zero-order spaces. *Theoretical Chemistry Accounts* **1997**, *98*, 57–63.
- (26) Holmes, A. A.; Tubman, N. M.; Umrigar, C. J. Heat-Bath Configuration Interaction: An Efficient Selected Configuration Interaction Algorithm Inspired by Heat-Bath Sampling. *Journal of Chemical Theory and Computation* **2016**, *12*, 3674–3680, PMID: 27428771.

- (27) Holmes, A. A.; Umrigar, C. J.; Sharma, S. Excited states using semistochastic heat-bath configuration interaction. *The Journal of Chemical Physics* **2017**, *147*, 164111.
- (28) Sharma, S.; Holmes, A. A.; Jeanmairet, G.; Alavi, A.; Umrigar, C. J. Semistochastic Heat-Bath Configuration Interaction Method: Selected Configuration Interaction with Semistochastic Perturbation Theory. *Journal of Chemical Theory and Computation* **2017**, *13*, 1595–1604.
- (29) Schriber, J. B.; Evangelista, F. A. Communication: An adaptive configuration interaction approach for strongly correlated electrons with tunable accuracy. *The Journal of Chemical Physics* **2016**, *144*, 161106.
- (30) Schriber, J. B.; Evangelista, F. A. Adaptive Configuration Interaction for Computing Challenging Electronic Excited States with Tunable Accuracy. *Journal of Chemical Theory and Computation* **2017**, *13*, 5354–5366, PMID: 28892621.
- (31) Liu, W.; Hoffmann, M. R. iCI: Iterative CI toward full CI. *Journal of Chemical Theory and Computation* **2016**, *12*, 1169–1178, PMID: 26765279.
- (32) Zhang, N.; Liu, W.; Hoffmann, M. R. Iterative Configuration Interaction with Selection. *Journal of Chemical Theory and Computation* **2020**, *16*, 2296–2316.
- (33) Coe, J. P. Machine Learning Configuration Interaction. *Journal of Chemical Theory and Computation* **2018**, *14*, 5739–5749, PMID: 30285426.
- (34) Tubman, N. M.; Lee, J.; Takeshita, T. Y.; Head-Gordon, M.; Whaley, K. B. A deterministic alternative to the full configuration interaction quantum Monte Carlo method. *The Journal of Chemical Physics* **2016**, *145*, 044112.
- (35) Tubman, N. M.; Freeman, C. D.; Levine, D. S.; Hait, D.; Head-Gordon, M.; Whaley, K. B. Modern Approaches to Exact Diagonalization and Selected Configuration

- Interaction with the Adaptive Sampling CI Method. *Journal of Chemical Theory and Computation* **2020**, *16*, 2139–2159.
- (36) Sugiyama, G.; Koonin, S. Auxiliary field Monte-Carlo for quantum many-body ground states. *Annals of Physics* **1986**, *168*, 1–26.
- (37) Al-Saidi, W. A.; Zhang, S.; Krakauer, H. Auxiliary-field quantum Monte Carlo calculations of molecular systems with a Gaussian basis. *The Journal of Chemical Physics* **2006**, *124*, 224101.
- (38) Zhang, S.; Krakauer, H. Quantum Monte Carlo Method using Phase-Free Random Walks with Slater Determinants. *Phys. Rev. Lett.* **2003**, *90*, 136401.
- (39) Booth, G. H.; Thom, A. J. W.; Alavi, A. Fermion Monte Carlo without fixed nodes: A game of life, death, and annihilation in Slater determinant space. *The Journal of Chemical Physics* **2009**, *131*, 054106.
- (40) Anderson, J. B. A random-walk simulation of the Schrödinger equation: H+3. *The Journal of Chemical Physics* **1975**, *63*, 1499–1503.
- (41) Klein, D. J.; Pickett, H. M. Nodal hypersurfaces and Anderson’s random-walk simulation of the Schrödinger equation. *The Journal of Chemical Physics* **1976**, *64*, 4811–4812.
- (42) Ceperley, D. M.; Alder, B. J. Quantum Monte Carlo for molecules: Green’s function and nodal release. *The Journal of Chemical Physics* **1984**, *81*, 5833–5844.
- (43) Cleland, D.; Booth, G. H.; Alavi, A. Communications: Survival of the fittest: Accelerating convergence in full configuration-interaction quantum Monte Carlo. *The Journal of Chemical Physics* **2010**, *132*, 041103.

- (44) Ghanem, K.; Lozovoi, A. Y.; Alavi, A. Unbiasing the initiator approximation in full configuration interaction quantum Monte Carlo. *The Journal of Chemical Physics* **2019**, *151*, 224108.
- (45) Petruzielo, F. R.; Holmes, A. A.; Changlani, H. J.; Nightingale, M. P.; Umrigar, C. J. Semistochastic Projector Monte Carlo Method. *Phys. Rev. Lett.* **2012**, *109*, 230201.
- (46) Blunt, N. S.; Smart, S. D.; Kersten, J. A. F.; Spencer, J. S.; Booth, G. H.; Alavi, A. Semi-stochastic full configuration interaction quantum Monte Carlo: Developments and application. *The Journal of Chemical Physics* **2015**, *142*, 184107.
- (47) Zhang, T.; Evangelista, F. A. A Deterministic Projector Configuration Interaction Approach for the Ground State of Quantum Many-Body Systems. *Journal of Chemical Theory and Computation* **2016**, *12*, 4326–4337, PMID: 27464301.
- (48) Greene, S. M.; Webber, R. J.; Weare, J.; Berkelbach, T. C. Beyond Walkers in Stochastic Quantum Chemistry: Reducing Error Using Fast Randomized Iteration. *Journal of Chemical Theory and Computation* **2019**, *15*, 4834–4850, PMID: 31390198.
- (49) Greene, S. M.; Webber, R. J.; Weare, J.; Berkelbach, T. C. Improved Fast Randomized Iteration Approach to Full Configuration Interaction. *Journal of Chemical Theory and Computation* **2020**, *16*, 5572–5585, PMID: 32697909.
- (50) Thom, A. J. W. Stochastic Coupled Cluster Theory. *Phys. Rev. Lett.* **2010**, *105*, 263004.
- (51) Filip, M.-A.; Scott, C. J. C.; Thom, A. J. W. Multireference Stochastic Coupled Cluster. *Journal of Chemical Theory and Computation* **2019**, *15*, 6625–6635, PMID: 31697497.
- (52) Filip, M.-A.; Thom, A. J. W. A hybrid stochastic configuration interaction–coupled cluster approach for multireference systems. *The Journal of Chemical Physics* **2023**, *158*, 184101.

- (53) Blunt, N. S.; Alavi, A.; Booth, G. H. Krylov-Projected Quantum Monte Carlo Method. *Phys. Rev. Lett.* **2015**, *115*, 050603.
- (54) Neufeld, V. A.; Thom, A. J. W. Accelerating Convergence in Fock Space Quantum Monte Carlo Methods. *Journal of Chemical Theory and Computation* **2020**, *16*, 1503–1510.
- (55) Blunt, N. S.; Smart, S. D.; Kersten, J. A. F.; Spencer, J. S.; Booth, G. H.; Alavi, A. Semi-stochastic full configuration interaction quantum Monte Carlo: Developments and application. *The Journal of Chemical Physics* **2015**, *142*, 184107.
- (56) Saad, Y. *Numerical Methods for Large Eigenvalue Problems*; Manchester University Press: Manchester, UK, 1992.
- (57) Blunt, N. S.; Thom, A. J. W.; Scott, C. J. C. Preconditioning and Perturbative Estimators in Full Configuration Interaction Quantum Monte Carlo. *Journal of Chemical Theory and Computation* **2019**, *15*, 3537–3551, PMID: 31050430.
- (58) Azad, A.; Buluc, A. A Work-Efficient Parallel Sparse Matrix-Sparse Vector Multiplication Algorithm. *Proceedings - 2017 IEEE International Parallel and Distributed Processing Symposium (IPDPS)* **2017**, 2017.
- (59) Lanczos, C. An iteration method for the solution of the eigenvalue problem of linear differential and integral operators. *Journal of research of the National Bureau of Standards* **1950**, *45*, 255–282.
- (60) Koch, E. In *The LDA+DMFT approach to strongly correlated materials*, Forschungszentrum Jülich; Pavarini, E., Koch, E., Vollhardt, D., Lichtenstein, A., Eds.; 2011.
- (61) Saad, Y. *Iterative methods for sparse linear systems*; SIAM, 2003.
- (62) Bai, Z.; Demmel, J.; Dongarra, J.; Ruhe, A.; van der Vorst, H. In *Templates for the*

- Solution of Algebraic Eigenvalue Problems*; Bai, Z., Demmel, J., Dongarra, J., Ruhe, A., van der Vorst, H., Eds.; Society for Industrial and Applied Mathematics, 2000.
- (63) Dargel, P. E.; Wöllert, A.; Honecker, A.; McCulloch, I. P.; Schollwöck, U.; Pruschke, T. Lanczos algorithm with matrix product states for dynamical correlation functions. *Phys. Rev. B* **2012**, *85*, 205119.
- (64) Musser, D. R. Introspective sorting and selection algorithms. *Software: Practice and Experience* **1997**, *27*, 983–993.
- (65) Werner, H.-J.; Knowles, P. J.; Knizia, G.; Manby, F. R.; Schütz, M. Molpro: a general-purpose quantum chemistry program package. *WIREs Computational Molecular Science* **2012**, *2*, 242–253.
- (66) <https://github.com/wlj89/SFCI>.
- (67) Chan, G. K.-L.; Kállay, M.; Gauss, J. State-of-the-art density matrix renormalization group and coupled cluster theory studies of the nitrogen binding curve. *The Journal of Chemical Physics* **2004**, *121*, 6110–6116.
- (68) Olivares-Amaya, R.; Hu, W.; Nakatani, N.; Sharma, S.; Yang, J.; Chan, G. K.-L. The ab-initio density matrix renormalization group in practice. *The Journal of Chemical Physics* **2015**, *142*, 034102.
- (69) Golub, G. H.; Van Loan, C. F. *Matrix Computations*, 3rd ed.; The Johns Hopkins University Press, 1996.